Regular Article

Conventional and inverse barocaloric effects around triple points in ferroelastics $(NH_4)_3NbOF_6$ and $(NH_4)_3TiOF_5$

M.V. Gorev [a,b], E.V. Bogdanov [a,c], I.N. Flerov [a,b,*]

[a] Kirensky Institute of Physics, Federal Research Center KSC SB RAS, 660036 Krasnoyarsk, Russia
[b] Institute of Engineering Physics and Radioelectronics, Siberian Federal University, 660074 Krasnoyarsk, Russia
[c] Institute of Engineering Systems and Energy, Krasnoyarsk State Agrarian University, 660049 Krasnoyarsk, Russia

A B S T R A C T

We report the conventional and inverse barocaloric effect (BCE) in ferroelastics $(NH_4)_3NbOF_6$ and $(NH_4)_3TiOF_5$. We found a rich set of the structural phase transitions and triple points on the $T - p$ phase diagrams. Extensive and intensive BCE near some transformations and around triple points in both crystals are outstanding ($|\Delta S_{BCE}^{max}| = 30$–$100$ J/kg·K; $|\Delta T_{AD}^{max}| = 4$–$22$ K) and can be achieved at low pressure 0.01–0.60 GPa.
PACS:
62.50.-p
65.40.-b
81.30.-t

Barocaloric effect (BCE) associated with the reversible change in the entropy/temperature, $\Delta S_{BCE} / \Delta T_{AD}$, under pressure variation under the isothermal/adiabatic conditions is a common caloric effect (CE) characteristic for substances of different physical nature in various aggregate states. This can be demonstrated using the Maxwell relation $(\partial S / \partial p)T = -(\partial V / \partial T)_p$ presented as follows

$$\Delta S_{BCE} = -\int_0^p \left(\frac{\partial V}{\partial T}\right)_p dp; \qquad \Delta T_{AD} = -\int_0^p \frac{T}{C_p}\left(\frac{\partial V}{\partial T}\right)_p dp \qquad (1)$$

where V is the volume, C_p is the heat capacity. In accordance with these equations, the values of both extensive, ΔS_{BCE}, and intensive, ΔT_{AD}, BCE strongly depend on a coefficient of the volume thermal expansion $\beta = V^{-1}(\partial V / \partial T)_p$. Solids under usual conditions show as a rule rather low value of β compared to gaseous materials used as refrigerants in the traditional vapor - compression systems. That is why for a long time BCE in solids has been studied to a much lesser extent than magneto(MCE)- and electro(ECE)-caloric effects in ferromagnets and ferroelectrics some of which are considered as potential solid refrigerants competitive in comparison with gaseous coolants [1–5]. However, near phase transitions where many properties of solids exhibit strongly anomalous behaviour, a value of the $(\partial V / \partial T)_p$ derivative can often vary by several orders of magnitude. In such a case both barocaloric characteristics,

ΔS_{BCE} and ΔT_{AD}, can reach very large magnitudes comparable with the highest values of extensive and intensive MCE and ECE [1–3]. Moreover, when heated through a point of the phase transition, the structural distortions may be accompanied by either increase or decrease in the unit cell volume. Thus, BCE can be either conventional, $(\partial V / \partial T)_p > 0$, associated with decrease in ΔS_{BCE} and increase in ΔT_{AD} under applying pressure or inverse, $(\partial V / \partial T)_p < 0$, $\Delta S_{BCE} > 0$ and $\Delta T_{AD} < 0$. The latter situation is less common than the former one. Nevertheless, inverse BCE was recently studied in ferroelectrics $BaTiO_3$, $(NH_4)_2SO_4$, NH_4HSO_4 and intermetallic compound La-Fe-Si-Co [6–9].

A different sign of the change of the unit cell volume is observed quite often at structural transformations in materials of the ferroelastic origin: fluorides, oxides and oxyfluorides with the perovskite-like structure [5,10]. Some of these crystals undergo at ambient pressure only one phase transition $G_0 \leftrightarrow G_1$ which is characterized by large entropy change ΔS and small change in the unit cell volume or in anomalous part of the β value. In such a case, in accordance with the Clausius–Clapeyron, $dT / dp = \delta V / \delta S$, and Ehrenfest, $dT / dp = T_0 \Delta \beta / \Delta C_p$, equations, baric coefficients dT_{G0-G1} / dp is also characterized by small magnitude. However, sometimes a splitting of the initial phase boundary is initiated by rather low pressure at the triple point, $p = p_{tr}$, with the appearance of the intermediate phase $G_0 \leftrightarrow G_{1'} \leftrightarrow G_1$. The entropy changes associated with each of the $G_0 \leftrightarrow G_{1'}$ and $G_{1'} \leftrightarrow G_1$ transitions are less than the entropy of the $G_0 \leftrightarrow G_1$ transformation at $p < p_{tr}$ and the following relationship occurs between these values $\Delta S_{G0-G1} = \Delta S_{G0-G1'} + \Delta S_{G1'-G1}$. The baric coefficients having different signs, $dT_{G0-G1'} / dp > 0$ and $dT_{G1'-G1} / dp < 0$, can increase in absolute value in the tens and hundreds of

times compared to dT_{G0-G1}/dp. To our knowledge, in spite of the growing interest to BCE in solids this effect is still unexplored near the triple points.

In the present letter, we investigate barocaloric properties of the two ferroelastic fluorine-oxygen compounds $(NH_4)_3NbOF_6$ and $(NH_4)_3TiOF_5$ with the elpasolite–cryolite structure [11–13]. At ambient pressure, niobate undergoes two structural phase transitions in a very narrow temperature range: $T_1 = 260$ K and $T_2 = 262$ K, whereas titanate shows only one ferroelastic phase transition at $T_0 = 264.7$ K. Entropy of the structural transformations was found very large in both oxyfluorides: in $(NH_4)_3NbOF_6$ $\Delta S_1 + \Delta S_2 = (8.5 + 30.3)$ J/mol·K and in $(NH_4)_3TiOF_5$ $\Delta S_0 = 18.1$ J/mol·K.

The dependences of $\Delta T_{AD}(T,p)$ and $\Delta S_{BCE}(T,p)$ were determined analyzing data on the heat capacity [11,12], the $T-p$ phase diagrams and the dependences of entropy of the phase transitions on temperature and pressure.

The $(NH_4)_3NbOF_6$ and $(NH_4)_3TiOF_5$ compounds were obtained from solution starting from high purity raw materials Nb_2O_5 (98.5%) and $(NH_4)_2TiOF_6$ (99%). The details of preparation were reported earlier [11,12]. XRD examination showed an absence of the secondary phases and revealed a cubic structure (sp. gr. Fm-3m) at room temperature in both oxyfluorides.

Differential thermal analysis (DTA) experiments under pressure were performed using home–made high–pressure chamber with multiplier [11]. A mixture of silicon oil and pentane exhibiting optimal electrical and heat conductivity, solidification point, and viscosity was used as a pressure-transmitting medium. To measure temperatures and anomalies of the heat capacity related to the phase transitions, we used the copper–constantan and high-sensitive differential copper–germanium thermocouples, respectively. The pressure was measured by a manganin resistive sensor. At ambient pressure, the samples of $(NH_4)_3NbOF_6$ and $(NH_4)_3TiOF_5$ show two and one anomalies in the DTA-signal, respectively, associated with two $G_0 \leftrightarrow G_1 \leftrightarrow G_2$ and single $G_0 \leftrightarrow G_1$ transformation at temperatures (Table 1), which coincide with the values observed in experiments with an adiabatic calorimeter [11,12].

Effect of pressure over a range of 0.0–0.5 GPa on the DTA-signals in the oxyfluorides $(NH_4)_3NbOF_6$ and $(NH_4)_3TiOF_5$ is illustrated in Figs. 1(a) and 2(a).

At pressure increase, both crystals demonstrate the splitting of the DTA-peaks observed at ambient pressure, which is connected with the appearance of the intermediate high-pressure phases. Considering temperatures of the DTA-peaks as temperatures of the phase transitions, we have built the $T-p$ phase diagrams (Figs. 1(b) and 2(b)). Common feature of both diagrams is connected with the triple points initiated by the rather low pressure. The coexistence of the G_1, $G_{1'}$ and G_2 phases in $(NH_4)_3NbOF_6$ was observed at the following coordinates $p_{tr1} = 0.07 \pm 0.01$ GPa, $T_{trp1} = 261.5 \pm 2$ K. Nonlinear phase boundaries in Fig. 1(b) can be described by the following equations: $T_{G0-G1} = 261 + 54p - 15p^2$, $T_{G1-G2} = 260.7 + 16p - 77p^2$, $T_{G1-G1'} = 260.3 + 19p - 27p^2$, $T_{G1'-G2} = 261.3 + 6p - 20p$ 2. The dT/dp values characterizing an initial slope of the phase boundaries, i.e. at $p = 0$ and $p = p_{tr1}$, are presented in Table 1. A sign of the baric coefficients $dT_{G1-G1'}/dp$ and dT_{G1-G2}/dp is changed at rather low pressure. Similar effect in perovskite–like ferroelstics [14] was explained by changes in the invariant of the

thermodynamic potential describing the interaction of the order parameter with the strain.

The $T-p$ phase diagram of $(NH_4)_3TiOF_5$ (Fig. 2(b)) shows five phase transitions between four crystal phases connected by two triple points: $p_{tr1} = 0.196 \pm 0.005$ GPa, $T_{tr1} = 265.7 \pm 0.5$ K, and $p_{tr2} = 0.291 \pm 0.005$ GPa, $T_{tr2} = 249.2 \pm 0.5$ K. Small value of dT_{G0-G1}/dp (Table 1) demonstrates a low sensitivity of the transformation $G_0 \leftrightarrow G_1$ to pressure. At triple point 1, the phase boundary $G_0 \leftrightarrow G_1$ splits into two lines associated with the succession of the two transformations: $G_0 \leftrightarrow G_2$ and $G_2 \leftrightarrow G_1$ characterized by very large values of dT/dp of the opposite sign. Further increase in pressure up to p_{tr2} leads to appearance of the two additional phase transitions: $G_1 \leftrightarrow G_3$ and $G_2 \leftrightarrow G_3$. Temperatures of the all phase transitions show strong linear dependence on the hydrostatic pressure. Due to the steep slope of the phase boundary $G_1 \leftrightarrow G_3$ the related transformation was observed in the narrow pressure-temperature range and its baric coefficient (Table 1) was determined with a rather large error.

The temperature dependences of the DTA-signal in Figs. 1(a) and 2(a) are equivalent to the temperature dependences of the anomalous heat capacity, $\Delta C_p(T)$, associated with the phase transitions. Therefore, the areas under the DTA-signal peaks can be considered as proportional to the entropies, ΔS_i, of the phase transitions. All the DTA-signal peaks in both oxyfluorides do not change the shape and area over the pressure range 0.0–0.5 GPa. A sum of the areas under peaks at $p > p_{tr}$ is equal to the area under the peak detected at $p < p_{tr}$ before splitting of the phase boundaries. Thus, entropies of the transformations in $(NH_4)_3NbOF_6$ and $(NH_4)_3TiOF_5$ are practically independent on pressure. We have normalized the areas under the DTA-signal peaks to the value of ΔS_i obtained in measurements of the heat capacity at ambient pressure using an adiabatic calorimeter [11,12] and determined dependences $\Delta S_i(T)$ at different pressure (Figs. 1(c) and 2(c)). The largest value of ΔS_{G2-G3} for $(NH_4)_3TiOF_5$ (Table 1) is associated with a contribution of entropy ΔS_{G1-G3} which was not observed at $p = 0$. In accordance with this point, the temperature dependence of $(\Delta S_{G2-G3} + \Delta S_{G0-G2})$ was shown in Fig. 2(b) beginning from zero whereas entropies ΔS_{G0-G1} and $(\Delta S_{G0-G2} + \Delta S_{G2-G1})$ were considered as additional contribution to ΔS_{G1-G3}.

Both extensive and intensive BCE in oxyfluorides were determined by the previously used method [15] using the data on heat capacity [11,12], the $T-p$ phase diagrams and temperature and pressure dependences of the phase transition entropies obtained in the present paper. Taking into account the negligible effect of the low pressure ($p \leq 0.5$ GPa) on ΔS_i (Figs. 1(a) and 2(a)), we suppose that lattice entropy, S_L, of fluorine-oxygen crystals with dominated ionic bonds also does not substantially depend on the hydrostatic pressure. The dependences $S_L(T) - S_L(100K)$ were obtained by integration of the $(C_L/T)(T)$ functions. C_L is the lattice heat capacity obtained by polynomial fitting of the experimental data outside the phase transition region. Temperature dependences of the total entropies under pressure (Figs. 1(d) and 2(d)) were determined by summation of the lattice entropy S_L and the anomalous contributions ΔS_i shifted along the temperature scale according to the appropriate sign and value of dT_i/dp (Table 1). In Fig. 2(d), the curve $S_L(T)$ at $p = 0.31$ GPa is shown in accordance with a difference between ΔS_i at $p = 0$ presented in Fig. 2(c). The behaviour of ΔS_{BCE} determined from temperature and pressure dependences of the total

Table 1
Barocaloric properties of $(NH_4)_3NbOF_6$ and $(NH_4)_3TiOF_5$ ferroelastics.

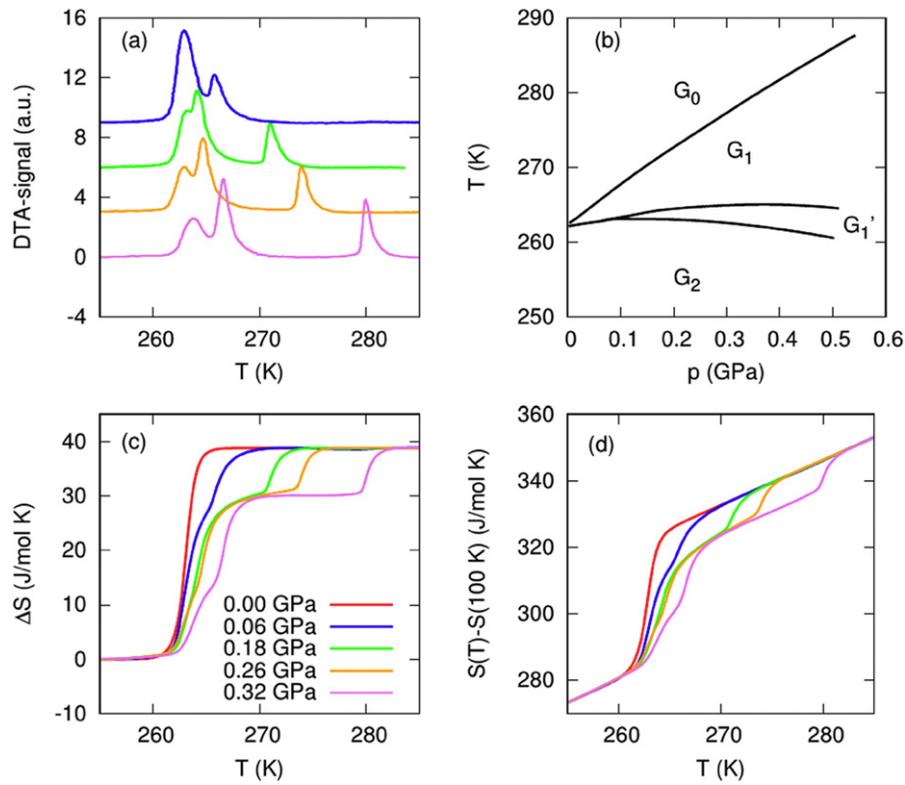| Crystal	$(NH_4)_3NbOF_6$				$(NH_4)_3TiOF_5$				
	G_0–G_1	G_1–G_2	G_1–$G_{1'}$	$G_{1'}$–G_2	G_0–G_1	G_0–G_2	G_2–G_1	G_2–G_3	G_1–G_3
T_i (K)	261	260			265				
dT_i/dp (K/GPa)	54	16	16	3	6.3	223	−176	−59	~ 425
ΔS_i (J/kg·K)	−31	−109	−36	−72	−85	−5.0	60	100	−36
ΔT_{AD}^{max} (K)	6.2	21.7	7.2	14.4	15.3	4.4	−11.5	−17.4	7
p_{min} (GPa)	0.11	1.35			2.4	$0.02 + p_{tr1}$	$0.06 + p_{tr2}$	$0.29 + p_{tr2}$	~0.01

Fig. 1. The dependence of (a) DTA-signal and (c) excess entropy ΔS on temperature at different hydrostatic pressure in $(NH_4)_3NbOF_6$; (b) $T - p$ phase diagram; (d) temperature dependence of total entropy of $(NH_4)_3NbOF_6$ at different hydrostatic pressure.

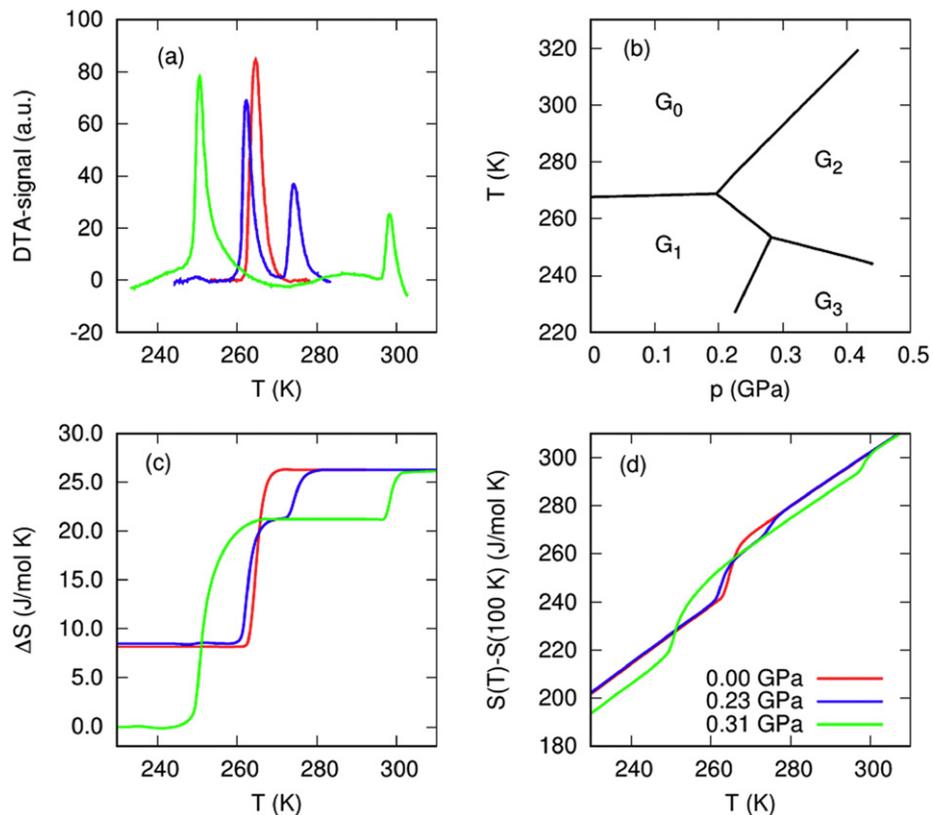**Fig. 2.** The dependence of (a) DTA-signal and (c) excess entropy ΔS on temperature at different hydrostatic pressure in $(NH_4)_3TiOF_5$; (b) $T - p$ phase diagram; (d) temperature dependence of total entropy of $(NH_4)_3TiOF_5$ at different hydrostatic pressure.

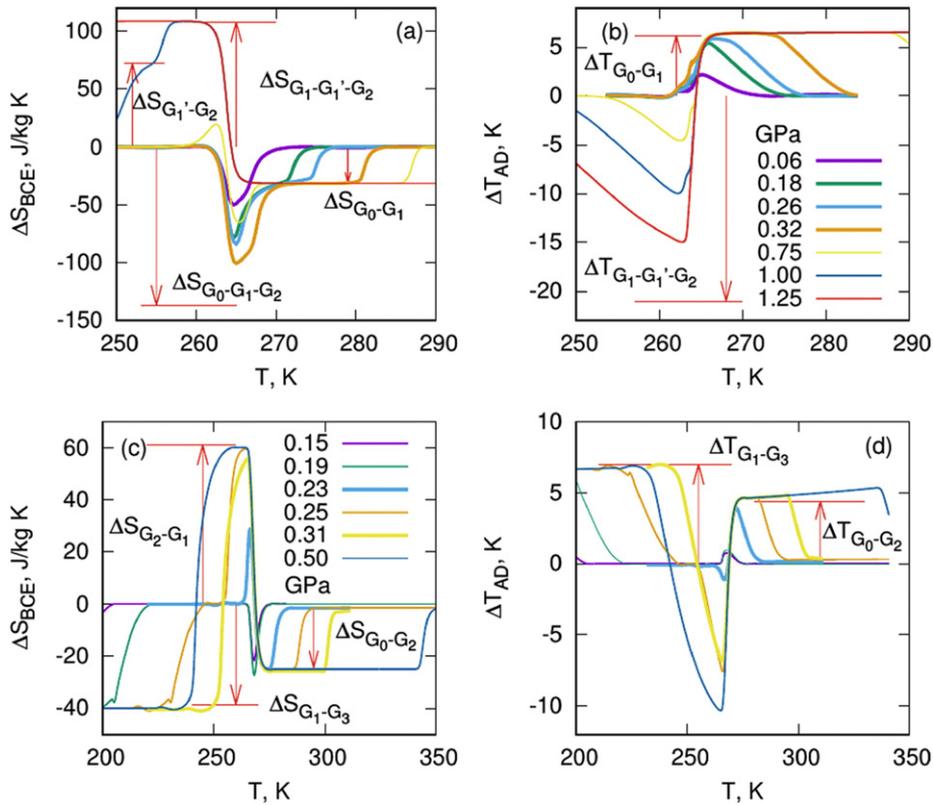**Fig. 3.** Temperature dependences of barocaloric entropy and temperature changes at different hydrostatic pressure: (a, b) in $(NH_4)_3NbOF_6$ and (c, d) in $(NH_4)_3TiOF_5$.

entropies $\Delta S_{BCE} = S(T,p) - S(T, p = 0)$ of $(NH_4)_3NbOF_6$ and $(NH_4)_3TiOF_5$ is shown in Fig. 3(a) and (c).

To obtain correct information on the behaviour of the intensive BCE, plots of $S(T,p) = S_L(T, p = 0) + \Delta S(T,p)$ were analyzed based on the condition of constant entropy $S(T,p) = S(T + \Delta T_{AD}, p = 0)$. By assuming the lattice entropy to be independent of rather low pressure, we determined the maximum possible values of extensive and intensive BCE for the phase transition. Both values are connected with entropy of the phase transition ΔS: $\Delta S_{BCE}^{max} = \Delta S$ and $\Delta T_{AD}^{max} = -T\Delta S / C_L$ [16]. One more important parameter of the barocaloric efficiency is a minimum pressure, $p_{min} = T\Delta S / C_L dT / dp$, required to implement both maximum BCE values. Barocaloric characteristics for the specific structural transformations are presented in Table 1.

Fig. 3 shows nontrivial behaviour of intensive and extensive BCE in both oxyfluorides which is associated with triple points on the $T - p$ phase diagrams. In $(NH_4)_3NbOF_6$ at $p = 0.06$ GPa $< p_{tr1}$, both phase transitions $G_0 \leftrightarrow G_1$ and $G_1 \leftrightarrow G_2$ contribute into ΔS_{BCE} and ΔT_{AD} (Fig. 3(a) and (b)), which appear as single peaks and are observed in the narrow temperature range.

A total entropy change associated with BCE is rather large ~50 J/kg·K (Fig. 3(a)). Further increase in pressure leads to two stage in the behaviour of BCE. Entropy $(\Delta SBCE)_{G0-G1}$ quickly reaches the maximum value at $p_{min} = 0.11$ GPa and remains constant. A contribution into ΔS_{BCE} connected with successive phase transitions $G_1 \leftrightarrow G_1' \leftrightarrow G_2$ was increased up to ~105 J/kg·K at $p = 0.32$ GPa. At this pressure the ΔT_{AD} reaches the maximum value. At $p > 0.32$ GPa there is a conversion of both BCE due to a change of the sign of $dT_{G1-G1'} / dp$ and $dT_{G1'-G2} / dp$ (Fig. 1(b)). Below $T_{G1'-G2}$, extensive and intensive BCE can reach 110 J/kg·K and -21 K, respectively, however, at rather high pressure, 1–2 GPa. Nevertheless, it is worth noting that there is a possibility to change entropy from -31 J/kg·K up to $+110$ J/kg·K and temperature from $+6$ K down to -21 K in very narrow temperature region, $\Delta T \approx 3$ K (Fig. 3(a) and (b)).

There are also two additional important peculiarities in the temperature-pressure behaviour of $(NH_4)_3NbOF_6$: firstly, very small difference $T_{G0-G1} - T_{G1-G2}$ at $p = 0$ and, secondly, very narrow interval of the pressure where the direct phase transition $G_1 \leftrightarrow G_2$ exists (Table 1 and Fig. 1(b)). These features can be used in the future to improve barocaloric properties of niobate by the following way. Based on dependencies $T_{G0-G1}(p)$ and $T_{G1-G2}(p)$, we have found that a triple point where the G_0, G_1 and G_2 phases may coexist could be observed at very low negative pressure $p_{tr2} < -0.01$ GPa. Such a small value p_{tr2} permits us to assume that the direct transformation $G_0 \leftrightarrow G_2$ can be realized by an increase in the unit cell volume as the result of a decrease in the internal (chemical) pressure. Such an effect can for example be achieved by partial cationic substitution of the NH_4 group by Cs atom because a stability of the crystal phases in the cubic fluorine and fluorine-oxygen compounds strongly depends on the size of cations and anions [10].

Due to a very low sensitivity of the phase transition $G_0 \leftrightarrow G_1$ in $(NH_4)_3TiOF_5$ to pressure, rather large maximum values of $(\Delta S_{BCE})_{G0-G1}$ and $(\Delta T_{AD})_{G0-G1}$ cannot be achieved because p_{min} is significantly higher than the pressure of both triple points (Table 1). In accordance with the dependence $S(T) - S(100$ K$)$ (Fig. 2(d)), titanate demonstrates conversion of BCE in two stages in rather narrow temperature range (Fig. 3(c) and (d)). At $p = 0.31$ GPa, above 268 K and below 255 K conventional BCE associated with the phase transitions $G_0 \leftrightarrow G_2$ and $G_1 \leftrightarrow G_3$, respectively, achieves the maximum at very low pressure (Table 1). In the region between the two triple points, rather low pressure, $p_{min} < p_{tr2}$, is needed to implement the greatest values of the inverse BCE (Table 1). Similar situation was observed at $p > p_{tr2}$, where BCE associated with the transformation $G_2 \leftrightarrow G_3$ remains inverse and shows gigantic maximum values of both $(\Delta S_{BCE})_{G2-G3}$ and $(\Delta T_{AD})_{G2-G3}$ at pressure, which can be implemented relatively easily (Table 1). One should also pay attention to a very low pressure needed to get $(\Delta S_{BCE}^{max})_{G1-G3}$ and $(\Delta T_{AD}^{max})_{G1-G3}$, which exist in a wide temperature range.

In the future it would be interesting to investigate the influence of chemical pressure on the $T - p$ phase diagram and barocaloric

parameters of titanium oxyfluoride. It can be assumed that the decrease in the unit cell volume caused for example by cationic substitution K^+ → NH_4^+ will shift both triple points to the lower external hydrostatic pressure. In such a case the most useful barocaloric parameters associated with successive phase transitions $G_0 \leftrightarrow G_2 \leftrightarrow G_1 \leftrightarrow G_3$ and $G_0 \leftrightarrow G_2 \leftrightarrow G_3$ can be achieved more easily.

In summary, this letter demonstrates BCE in oxyfluorides $(NH_4)_3NbOF_6$ and $(NH_4)_3TiOF_5$ undergoing structural phase transitions near room temperature. The $T - p$ phase diagrams show triple points and crystal phases induced by high pressure. Entropy of the phase transformations was found to be independent on pressure, at least up to 0.5 GPa. BCE observed around the triple points demonstrate options worthy of attention and are comparable with the caloric parameters of the known solid refrigerants of different origin [1–3,17]. In both compounds, the conversion from the conventional BCE to the inverse is observed in very narrow temperature range and followed by gigantic change of both $|\Delta S_{BCE}|$ and $|\Delta T_{AD}|$. The possibility of improving the barocaloric properties by changing the chemical pressure is discussed.

Acknowledgements

References

[1] K.A. GschneidnerJr, V.K. Pecharsky, A.O. Tsokol, Rep. Prog. Phys. 68 (2005) 1479–1539 http://stacks.iop.org/0034-4885/68/i=6/a=R04.

[2] M. Valant, Prog. Mater. Sci. 57 (2012) 980–1009, http://dx.doi.org/10.1016/j.pmatsci.2012.02.001.

[3] X. Moya, S. Kar-Narayan, N.D. Mathur, Nat. Mater. 13 (2014) 439–450.

[4] I.N. Flerov, M.V. Gorev, E.V. Bogdanov, N.M. Laptash, Ferroelectrics 500 (2016) 153–163, http://dx.doi.org/10.1080/00150193.2016.1214525.

[5] I.N. Flerov, M.V. Gorev, M.S. Molokeev, N.M. Laptash, Photonic and Electronic Properties of Fluoride Materials: Progress in Fluorine Science Series, Elsevier, 2016 355–381, http://dx.doi.org/10.1016/B978-0-12-801639-8.00016-7.

[6] E. Stern-Taulats, P. Lloveras, M. Barrio, E. Defay, M. Egilmez, A. Planes, J.-L. Tamarit, L. Mañosa, N.D. Mathur, X. Moya, APL Mater. 4 (2016), 091102. http://dx.doi.org/10.1063/1.4961598.

[7] P. Lloveras, E. Stern-Taulats, M. Barrio, J.-L. Tamarit, S. Crossley, W. Li, V. Pomjakushin, A. Planes, L. Mañosa, N.D. Mathur, X. Moya, Nat. Commun. 6 (2015) 8801, http://dx.doi.org/10.1038/ncomms9801.

[8] E.A. Mikhaleva, I.N. Flerov, A.V. Kartashev, M.V. Gorev, E.V. Bogdanov, V.S. Bondarev, Solid State Sci. 67 (2017) 1–7, http://dx.doi.org/10.1016/j.solidstatesciences.2017.03.004.

[9] L. Mañosa, D. González-Alonso, A. Planes, M. Barrio, J.-L. Tamarit, I.S. Titov, M. Acet, A. Bhattacharyya, S. Majumdar, Nat. Commun. 2 (2011) 595, http://dx.doi.org/10.1038/ncomms1606.

[10] I.N. Flerov, M.V. Gorev, K.S. Aleksandrov, A. Tressaud, J. Grannec, M. Couzi, Mater. Sci. Eng. R. Rep. 24 (1998) 81–151, http://dx.doi.org/10.1016/S0927-796X(98)00015-1.

[11] I.N. Flerov, M.V. Gorev, V.D. Fokina, A.F. Bovina, N.M. Laptash, Phys. Solid State 46 (2004) 915–921, http://dx.doi.org/10.1134/1.1744971.

[12] V.D. Fokina, I.N. Flerov, M.V. Gorev, E.V. Bogdanov, A.F. Bovina, N.M. Laptash, Phys. Solid State 49 (2007) 1548–1553, http://dx.doi.org/10.1134/S1063783407080240.

[13] A. Udovenko, N. Laptash, I. Maslennikova, J. Fluor. Chem. 124 (2003) 5–15, http://dx.doi.org/10.1016/S0022-1139(03)00166-0.

[14] I.N. Flerov, M.V. Gorev, K.S. Aleksandrov, Ferroelectrics 169 (1995) 199–205, http://dx.doi.org/10.1080/00150199508217330.

[15] M.V. Gorev, I.N. Flerov, E.V. Bogdanov, V.N. Voronov, N.M. Laptash, Phys. Solid State 52 (2010) 377–383, http://dx.doi.org/10.1134/S1063783410020253.

[16] R. Pirc, Z. Kutnjak, R. Blinc, Q.M. Zhang, Appl. Phys. Lett. 98 (2011), 021909. http://dx.doi.org/10.1063/1.3543628.

[17] L. Mañosa, A. Planes, Adv. Mater. 29 (2017) 1603607, http://dx.doi.org/10.1002/adma.201603607.